

SCIENTIFIC REPORTS



OPEN

Tunable liquid crystal multifocal microlens array

José Francisco Algorri¹, Noureddine Bennis², Virginia Urruchi¹, Przemek Morawiak², José Manuel Sánchez-Pena¹ & Leszek R. Jaroszewicz²

A novel liquid crystal microlens array with tunable multifocal capability, high optical power and fill-factor is proposed and experimentally demonstrated. A specific hole pattern design produces a multifocal array with only one voltage control. Three operations modes are possible, “Off”, “Tunable Multifocal” and “Unifocal”. The design is patterned in both substrates. Then, the substrates are arranged in symmetrical configuration. The result is a high optical power in comparison with typical hole patterned structures. Besides, it is proposed a hexagonal pattern that produces a high fill factor, specially indicated for some applications as Integral Imaging. The array has several useful characteristics for this type of application: tunability for the loss of resolution; multifocal for extended DOF; high fill factor to increase the number of views; and low power consumption for integration in portable devices. Moreover, the optical characteristics of the proposed device could bring new applications in other fields.

Research on liquid crystal (LC) lenses has gained an increasing interest in recent years. The low-weight, tunable focus, low power consumption and broad range of applications makes them unique with respect to other technologies. Since the first LC lens was proposed by Berreman *et al.*¹ and Sato *et al.*² several decades ago, a lot of different structures have come up. Some of the most important are, patterned electrodes^{3,4} Fresnel lenses⁵, modal control^{6,7} and immersed microlenses⁸. Another option is to modify the LC mixture itself. For example, polymer networks⁹, concentration redistribution¹⁰, carbon nanotubes¹¹, blue-phase LC¹², dual frequency LC¹³, tunable frequency¹⁴. This last option, is used to improve the switching time of the LC. Polymer networks and blue phases (a special cholesteric LC phase), have microsecond response time but the optical phase modulation is very limited. Dual frequency and tunable frequency improve both characteristics. Some recent applications of LC lenses include, auto-focusing systems and optical zoom systems¹⁵, pico-projection systems¹⁶, correction of defects in holographic projection systems¹⁷, photovoltaics¹⁸ or bio-optics (endoscopy¹⁹, ophthalmology^{20,21}). Another important application is also 3D vision²². The research on LC lenses for autostereoscopic vision has produced several interesting results²³. Liquid crystal lenses can be used as a replacement of conventional arrays in spatial multiplexing technique. This technique is based on classical optical phenomena as diffraction, reflection, refraction and occlusion in order to deviate the images to different positions in front of the display. Several technologies to produce this effect have been proposed. Among them, occlusive and refractive elements are the most used. Occlusive elements usually consists on masks containing vertical apertures that cover the light at certain angles. On the other hand, refractive elements are based on microlenses, with the advantage of more brightness, view angle and less crosstalk (depending on the microlens quality). These techniques, which are already used in commercial products, have not produced enough interest in the users. Some reasons are the reduced 3D content, low qualities (producing crosstalk) and the key problem of vergence-accommodation conflict (the adjustment of the eye focus). In order to avoid this problem, several solutions have been proposed. For example, increase the number of views or use full parallax (multi-view²⁴ or Integral Imaging²⁵). Integral imaging (InI) have both characteristics, several views and full parallax, making it the most promising technology for autostereoscopic displays and cameras. Gabriel M. Lippmann proposed this technique in 1908. He used an array of microlenses to collect the scene information in several tiny versions of the same one, each one with a different angle and position (similar to have a sampled hologram). The scene can be reproduced by using also microlenses, in this case the reproduction have full parallax and the cue of accommodation. This makes the system one of the best solutions to reproduce 3D images without visual strain and fatigue. Thanks to current developments on microlens manufacturing, this technique has been exploited recently with the commercialization of the first plenoptic camera²⁶. These types of cameras have several advantages e.g. rendering images of several views, digital refocusing, depth estimation, 3D reconstruction,

¹Department of Electronic Technology, Carlos III University, Madrid, 28911, Spain. ²New Technologies and Chemistry Faculty, Military University of Technology, Warsaw, 00-908, Poland. Correspondence and requests for materials should be addressed to J.F.A. (email: jalgorri@ing.uc3m.es)

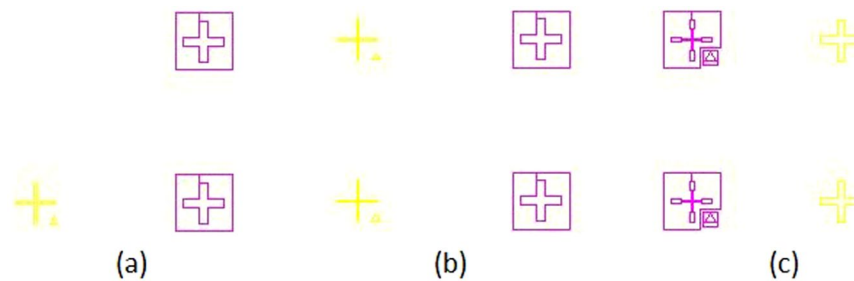


Figure 1. Sample of the used motif for align the two substrates.

etc. Despite this, the use of fixed microlenses has several limitations due to the lack of tuning. In the literature, it is possible to find several proposals to solve these problems, for example an extended Depth of Field (DOF) was proposed in²⁷ by using a multifocal fixed lens. For the loss of resolution, switchable LC lenses were proposed in²⁸. The DOF has been demonstrated to be tunable in²⁹ and³⁰. In³¹ LC microlenses were proposed in order to increase the viewing angle or field of view (FOV).

In this work, a novel tunable multifocal microlens array is proposed and experimentally demonstrated. The tunability is based on the properties of LC materials. Three operations modes are possible, OFF, tunable multifocal and unifocal. These modes can be controlled with only one low voltage signal. Among others, one possible application could be InI. The array has several useful characteristics for this type of application: tunability for the loss of resolution; multifocal for extended DOF; high fill factor for increase the number of views; and low power consumption for integration in portable devices. Moreover, the optical characteristics of this device could bring new applications in other fields

Design and Structure

Conventional lenses have two physical characteristics that modify a wavefront through them, the contrast between the refractive index of the lens and the surrounding medium, and the curvature of the interface between them. In the case of LC lenses, the medium is non-homogeneous, in consequence the wavefronts decrease its speed in the optically dense regions and are accelerated in areas of lower density. Because LC lenses are actually GRaded Index (GRIN) lenses, the estimation of the focal length, f_{GRIN} , of the LC lenses is simple if the focusing of parallel rays is considered (Eq. 1),

$$f_{GRIN} = \frac{r^2}{2 \cdot t \cdot (n_{max} - n(r))} \quad (1)$$

where R is the lens radius (half lens pitch), t is the thickness of the lens (thickness of the LC layer) and $n_{max} - n(r)$ is the difference between the maximum refractive index, n_{max} (at the optical axis of each lens) and the refractive index at the position r (that is, at the edge of the lens). In order to change the focal length, two structural parameters can be modified, the radius and the thickness. In this work, several focal lengths are created by varying the radius of each microlens. If more contrast ratio between focal lengths would be required, the thickness could be also modified (by depositing photoresist of different thicknesses).

Symmetrical electrodes are used in order to increase the optical power, for this reason, special mask patterns have to be designed. Each square of the mask device is patterned with a specific motif (see Fig. 1),

The fabrication process requires a precise alignment of both upper and bottom substrates. Motifs of Fig. 1 allow alignments in the limit of the mask aligner. A mask aligner MA/BA6 Mask and Bond Aligner have been used. The MA/BA6 is equipped with a motorized top side alignment system that can reach an alignment accuracy of $\pm 0.5 \mu\text{m}$. To reduce diffraction effects at the edge of the structured patterns, contact mode is used. In this process, the mask and the wafer are pressed all together. The same mask aligner has been used to align the top and the bottom hexagonal pattern before assembly the microlens device. Two ITO coated substrates ($20 \Omega/\text{sq}$) with hexagonal electrodes patterned in each one Fig. 2(a) are prepared. This hexagonal aperture produces the hexagonal type microlenses. A polyimide (PIA2000) is deposited over the two substrates to have certain molecular alignment. Spacers of $40 \mu\text{m}$ diameter, mixed with optical glue, are deposited to separate the two substrates. Finally, a LC (E7) fills the cavity. The electro-optical parameters are: $n_e = 1.7305$; $n_o = 1.5189$ ($\Delta n = 0.2116$ at 633 nm , 25°C)³². The diameters of the hexagons range from 120 to $90 \mu\text{m}$ in steps of $10 \mu\text{m}$. The total active area of the array is 2.13 cm width and 1.42 cm height.

In order to have a high fill factor, microlenses with hexagonal apertures are designed. This allows a considerably reduction of the space between them. The symmetrical configuration produces a high optical power as it is demonstrated in the results. In comparison with typical hole lenses with the same aperture and thickness, the optical power is doubled. The use of symmetrical electrodes avoid the negative effect of a continuous ground electrode. When one substrate have 0 volts, the voltage distribution in most part of the LC material is below threshold voltage. For this reason, in asymmetrical configuration an insufficient use of the LC birefringence is made. The symmetrical electrodes produce voltages above the threshold voltage in the center of the microlenses. Thanks to this effect, the molecules are switched on in this region producing higher birefringence differences. In consequence, the phase difference with a symmetrical configuration is considerable higher. The main advantage

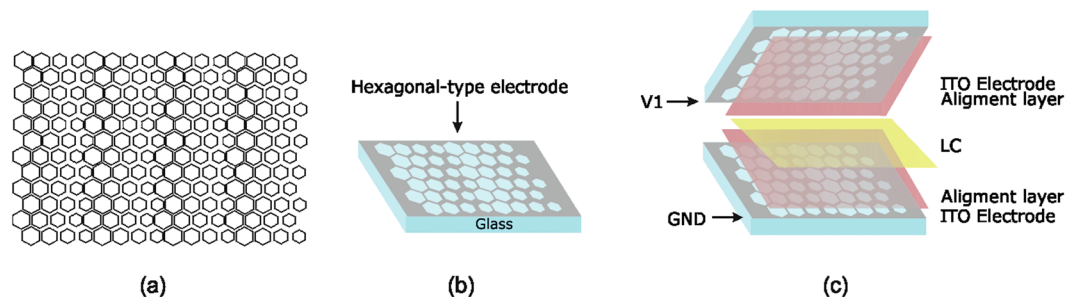


Figure 2. Tunable LC microlens array. (a) Hexagonal patterns for the mask, (b) depiction of one substrate, (c) depiction of the microlens array composition.

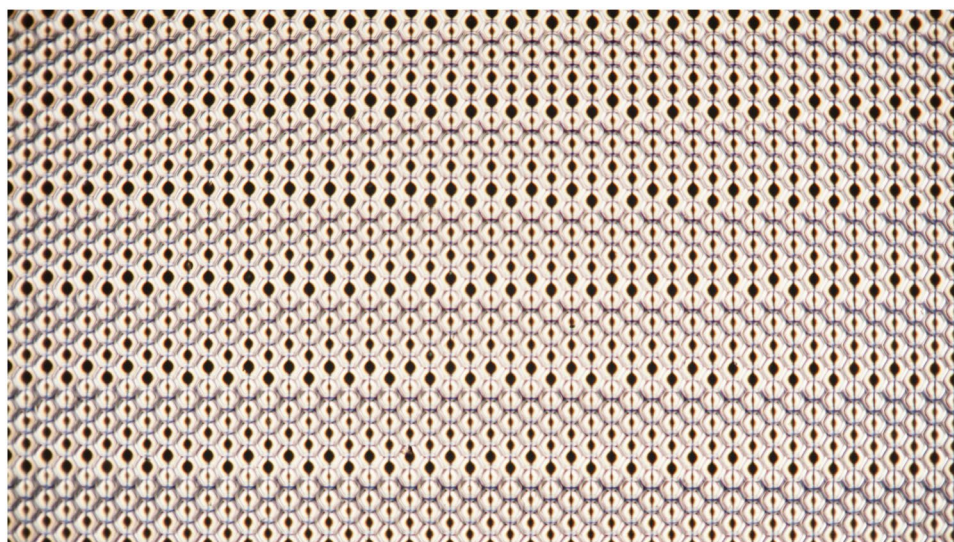


Figure 3. Experimental light intensity measurement by using a polarized microscope ($\times 5$). The applied voltage is $3 V_{\text{RMS}}$.

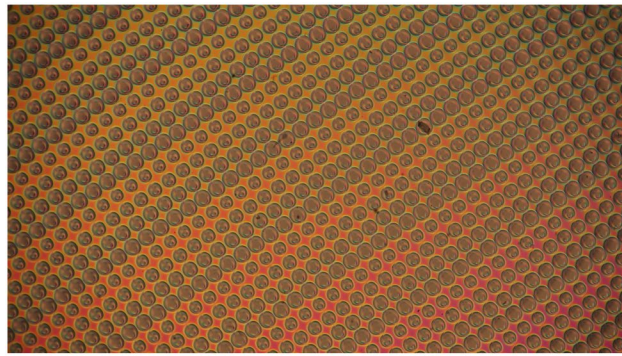
of the proposed device is that only one voltage source is required. Moreover, low voltage signals are enough to switch the microlenses. Extended results are described in the next section.

Experimental set-up and Results

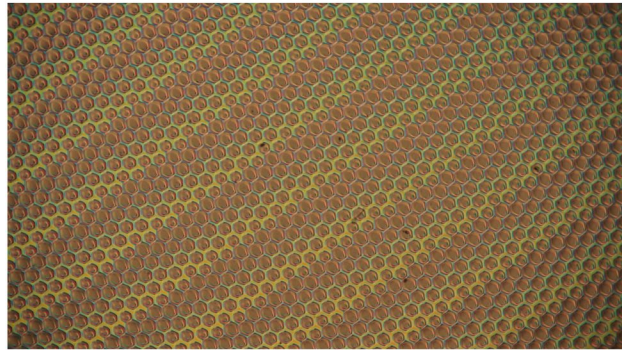
In order to demonstrate the homogeneity and the fill factor of the whole sample, Fig. 3 shows the switched sample by using a polarized microscope ($\times 5$ objective) and Fig. 4a comparison between the use of circular and hexagonal apertures.

The homogeneity of the sample is clearly stated. The fill factor is higher in the hexagonal pattern as the spaces between circles is avoided. The multifocal property can be observed through the different spot sizes. View that is more detailed is obtained through the fringe patterns. For this experiment, the system is placed in an optical table. The experimental set-up consists of: a He-Ne laser source (632.8 nm), a neutral density filter, a LC sample between crossed polarizers, a $\times 10$ microscope objective and a B/W CCD digital camera (effective no. of pixels 1344×1024).

Figure 5 shows the experimental fringe patterns of the proposed device for several applied voltages. Every two bright fringes means an optical phase difference of 2π between them. Thanks to this, the phase profile and the focal length can be extracted from these results³³. As can be observed, the lower the voltage the lower the number of fringes. This means that low optical power is obtained, generating a higher focal distance. From these observations three operations modes are expected. If the voltage do not reach $1.2 V_{\text{RMS}}$, the molecules are below threshold voltage and parallel to the substrate, in consequence there is not birefringence difference from the side to the center of the microlenses. This would be the “Off” mode. When the voltage is increased, the molecules start to switch in the sides, remaining parallel to the substrate in the center, and then the fringe patterns appear. Until $2.6 V_{\text{RMS}}$ the number of fringes is almost the same for the four type of microlens, $120 \mu\text{m}$ (A), $110 \mu\text{m}$ (B), $100 \mu\text{m}$ (C) and $90 \mu\text{m}$ (D). In this case, as the only parameter of Eq. 1 that changes is r , the focal distance changes in quadratic proportion. A multifocal tunable lens is obtained in this range (“Tunable Multifocal” mode). Moreover, the aperture is almost circular (see Fig. 4b and c). The elastic forces for these voltages are relatively low, the molecules have a smooth directional transition between them so the hexagonal aperture is almost circular. The last tunable range

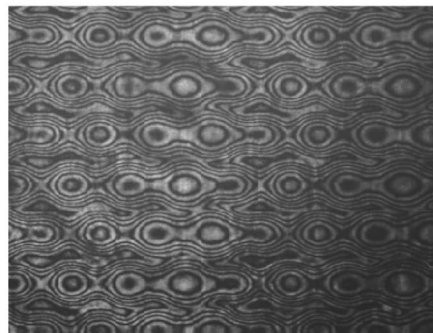


(a)

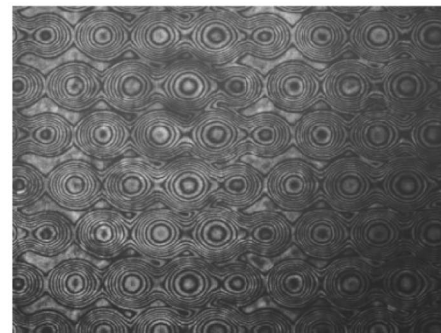


(b)

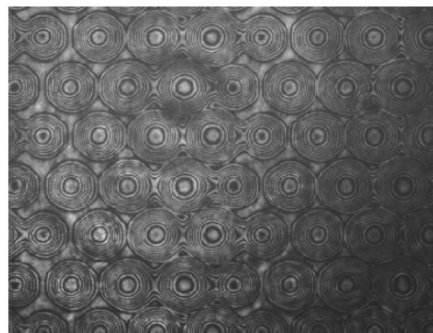
Figure 4. Experimental light intensity measurement between crossed polarizers and the sample at 45° for (a) circular apertures and (b) hexagonal. The applied voltage is $3 V_{\text{RMS}}$.



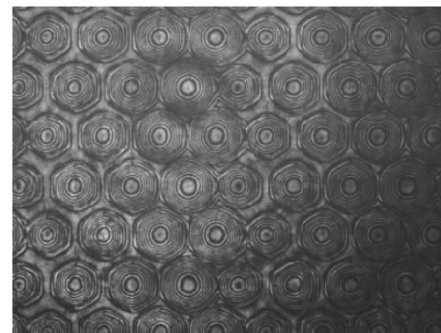
(a)



(b)



(c)



(d)

Figure 5. Experimental interference fringes patterns for different voltages, (a) $1.8 V_{\text{RMS}}$, (b) $2.2 V_{\text{RMS}}$, (c) $2.6 V_{\text{RMS}}$, (d) $2.8 V_{\text{RMS}}$.

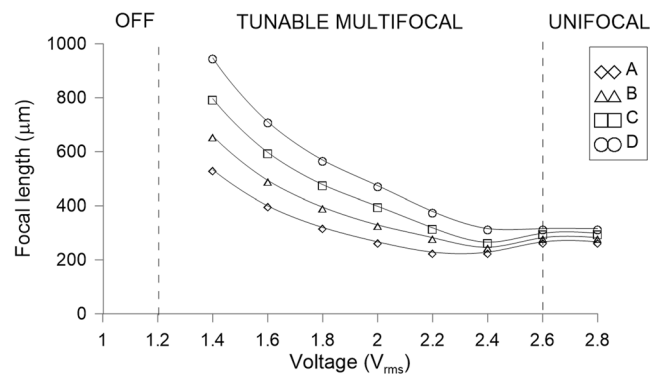


Figure 6. Resulting focal distances for microlenses with diameters of 120 μm (A), 110 μm (B), 100 μm (C) and 90 μm (D).

can be considered above $2.6 V_{RMS}$, two combined physical effects makes the lenses (A, B, C, D) to have the same focal length. Despite the radius is different, the number of fringes is also different. In this case, there is a limit of the maximum phase profile that can be obtained related to the ratio between the radius and thickness of the LC microlens³⁴. The higher the radius the higher the birefringence difference. Both terms are offset against each other in Eq. 1, The result is a similar focal length in each microlens (“Unifocal” mode). In order to observe these effects, the focal length of each microlens for several voltages is plotted in Fig. 6.

As it was observed in the fringe patterns, there is a modulation region between the threshold voltage and $2.4 V_{RMS}$ (“Tunable Multifocal” mode). The maximum focal length ratio is 56% for $1.4 V_{RMS}$, with a focal length ranging from 948 μm to 533 μm . For voltages above $2.6 V_{RMS}$ the focal length, converge around 300 μm (“Unifocal” mode). As commented before, despite the radius is different, the number of fringes is also different so both terms compensate each other in Eq. 1.

In³¹ it was demonstrated a control of the FOV and the Multiview image processing with LC lenses. In this case, this multifocal lens array would be capable of the DOF control with the added advantage of extension of the same one²⁷. In addition, full resolution can be obtained in the OFF mode.

Conclusions

A novel LC microlens array with multifocal capability, high optical power and almost full fill-factor has been proposed and experimentally demonstrated. The combination of a specific hole pattern design produces a multifocal array with only one voltage control. Three operations modes are possible, OFF, tunable multifocal and unifocal. Symmetrical electrodes are used. The result is a high optical power in comparison with typical hole patterned structures. Besides, it is proposed a hexagonal pattern that produces a high fill factor, specially indicated for some applications as Integral Imaging. The array has several useful characteristics for this type of application, tunability for the loss of resolution, multifocal for extended DOF, high fill factor for increase the number of views, and low power consumption for integration in portable devices. Moreover, the optical characteristics of this novel device could bring novel applications in other fields.

References

- Berreman, D. W. Variable-focus LC-lens system. Bell Telephone Laboratories, United States patent US 4190330 (1980).
- Sato, S. Liquid-crystal lens-cells with variable focal length. *Jpn. J. Appl. Phys.* **18**, 1679–1684 (1979).
- Nose, T. & Sato, S. A liquid crystal microlens obtained with a non-uniform electric field. *Liq. Cryst.* **5**, 1425–1433 (1989).
- Algorri, J. F., Urruchi, V., Bennis, N., Sánchez-Pena, J. M. & Otón, J. M. Cylindrical Liquid Crystal Microlens Array with Rotary Optical Power and Tunable Focal Length. *IEEE Elect. Dev. Lett.* **36**, 582–584 (2015).
- Williams, G., Powell, N., Purvis, A. & Clark, M. G. Electrically controllable liquid crystal fresnel lens. In *Opto-electronics Symposium SPIE 1168* (1989).
- Love, G. D. & Naumov, A. F. Modal liquid crystal lenses. *Liq. Cryst. Today* **10**, 1–4 (2000).
- Loktev, M. Y. *et al.* Wave front control systems based on modal liquid crystal lenses. *Rev. Sci. Instrum.* **71**, 3290–3297 (2000).
- Dai, H. T., Liu, Y. J., Sun, X. W. & Luo, D. A negative-positive tunable liquid-crystal microlens array by printing. *Opt. Express* **17**, 4317–4323 (2009).
- Ren, H. & Wu, S.-T. Tunable electronic lens using a gradient polymer network liquid crystal. *Applied Physics Letters* **82**, 22 (2003).
- Ren, H., Lin, Y.-H. & Wu, S.-T. Adaptive lens using liquid crystal concentration redistribution. *Applied Physics Letters* **88**, 191116 (2006).
- Rajasekharan, R. *et al.* Optimization of nanotube electrode geometry in a liquid crystal media from wavefront aberrations. *Applied Optics* **51**, 422 (2012).
- Lin, S.-H., Huang, L.-S., Lin, C.-H. & Kuo, C.-T. Polarizer-free and fast response microlens arrays using polymer-stabilized blue phase liquid crystals. *Applied Physics Letters* **96**, 113505 (2010).
- Xianyu, H., Wu, S.-T. & Lin, C.-L. Dual frequency liquid crystals: a review. *Liquid Crystals* **36**, (2009).
- Algorri, J. F. *et al.* Low aberration and fast switching microlenses based on a novel liquid crystal mixture. *Opt. Express* **25**, 14795–14808 (2017).
- Ye, M. *et al.* Focus tuning by liquid crystal lens in imaging system. *Appl. Opt.* **51**, 7630–5 (2012).
- Lin, Y.-H. & Chen, M.-S. A pico projection system with electrically tunable optical zoom ratio adopting two liquid crystal lenses. *J. Disp. Technol.* **8**, 401–404 (2012).
- Lin, H.-C., Collings, N., Chen, M.-S. & Lin, Y.-H. A holographic projection system with an electrically tuning and continuously adjustable optical zoom. *Opt. Express* **20**, 27222–9 (2012).

18. Tsou, Y.-S., Chang, K.-H. & Lin, Y.-H. A droplet manipulation on a liquid crystal and polymer composite film as a concentrator and a sun tracker for a concentrating photovoltaic system. *J. Appl. Phys.* **113**, 244504 (2013).
19. Hassanfiroozi, A., Huang, Y.-P., Javidi, B. & Shieh, H.-P. D. Hexagonal liquid crystal lens array for 3D endoscopy. *Opt. Express* **23**, 971–81 (2015).
20. Pixeloptics, Adjustable electro-active optical system and uses thereof. US patent 20140204333 A1 (2014).
21. Lin, Y.-H. & Chen, H.-S. Electrically tunable-focusing and polarizer-free liquid crystal lenses for ophthalmic applications. *Opt. Express* **21**, 9428–36 (2013).
22. Algorri, J. F., Urruchi, V., Sánchez-Pena, J. M. & Otón, J. M. An Autostereoscopic Device for Mobile Applications Based on a Liquid Crystal Microlens Array and an OLED Display. *J. Disp. Technol.* **46**, 327–336 (2014).
23. Algorri, J. F., Urruchi, V., García-Cámara, B. & Sánchez-Pena, J. M. Liquid crystal microlenses for autostereoscopic displays. *Materials* **9**, 1–17 (2016).
24. Dodgson, N. A. Optical devices: 3D without the glasses. *Nature* **495**, 316–7 (2013).
25. Xiao, X., Javidi, B., Martínez-Corral, M. & Stern, A. Advances in three-dimensional integral imaging: sensing, display, and applications. *Appl. Opt.* **52**, 546–60 (2013).
26. Adelson, E. H. & Wang, J. Y. A. Single Lens Stereo with Plenoptic Camera. *IEEE Transactions on Pattern Analysis and Machine Intelligence* **14**(2), 99–106 (1992).
27. Georgiev, T. G. Plenoptic camera with large depth of field. US 7949252 B1 (2011).
28. Kwon, H. *et al.* A Gradient Index Liquid Crystal Microlens Array for Light-Field Camera Applications. *Phot. Techn. Lett.* **27**, 836–839 (2015).
29. Lei, Y. *et al.* An electrically tunable plenoptic camera using a liquid crystal microlens array. *Rev. Sci. Instr.* **86**, 053101 (2015).
30. Shen, X. *et al.* Extended depth-of-focus 3D micro integral imaging display using a bifocal liquid crystal lens. *Opt. Lett.* **40**, 538–541 (2015).
31. Algorri, J. F. *et al.* Integral imaging capture system with tunable field of view based on liquid crystal microlenses. *IEEE Photon. Technol. Lett.* **28**, 1854–1857 (2016).
32. Li, J., Wen, C.-H., Gauza, S., Lu, R. & Wu, S.-T. Refractive indices of liquid crystals for display applications. *Journal of Display Technology* **1**, 51–61 (2005).
33. Urruchi, V. *et al.* Lenticular Arrays Based on Liquid Crystals. *Opto-electron. Rev.* **20**(3), 38–44 (2012).
34. Algorri, J. F., Urruchi, V., Bennis, N. & Sánchez-Pena, J. M. Using an Analytical Model to Design Liquid Crystal Microlenses. *IEEE Photon. Technol. Lett.* **26**(8), 793–796 (2014).

Acknowledgements

This work was supported by the Research and Development Program through the Comunidad de Madrid (SINFOTON S2013/MIT-2790), the Ministerio de Economía y Competitividad of Spain (TEC2013-47342-C2-2-R) and the funding from Agencia Estatal de Investigación (AEI) and Fondo Europeo de Desarrollo Regional (FEDER) for the Project TEC2016-77242-C3-1-R AEI/FEDER,UE. Finally, N. Bennis, P. Morawiak and L. R. Jaroszewicz, thank the Polish Ministry of Science and Higher Education (Statutory Activity PBS-654 of Military University of Technology).

Author Contributions

J.F. Algorri and N. Bennis designed the device and the electrical waveforms. N. Bennis and P. Morawiak fabricated the device. J.F. Algorri, V. Urruchi and N. Bennis analyzed the data, wrote the main manuscript text and prepared the figures. J.M. Pena and L.R. Jaroszewicz supervised the work.

Additional Information

Competing Interests: The authors declare that they have no competing interests.

Publisher's note: Springer Nature remains neutral with regard to jurisdictional claims in published maps and institutional affiliations.



Open Access This article is licensed under a Creative Commons Attribution 4.0 International License, which permits use, sharing, adaptation, distribution and reproduction in any medium or format, as long as you give appropriate credit to the original author(s) and the source, provide a link to the Creative Commons license, and indicate if changes were made. The images or other third party material in this article are included in the article's Creative Commons license, unless indicated otherwise in a credit line to the material. If material is not included in the article's Creative Commons license and your intended use is not permitted by statutory regulation or exceeds the permitted use, you will need to obtain permission directly from the copyright holder. To view a copy of this license, visit <http://creativecommons.org/licenses/by/4.0/>.

© The Author(s) 2017